Diffusion Measurements by Electrospray Mass Spectrometry for Studying Solution-Phase Noncovalent Interactions

Sonya M. Clark and Lars Konermann
Department of Chemistry, The University of Western Ontario, London, Ontario, Canada

This study describes a novel approach for monitoring noncovalent interactions in solution by electrospray mass spectrometry (ESI-MS). The technique is based on measurements of analyte diffusion in solution. Diffusion coefficients of a target macromolecule and a potential low molecular weight binding partner are determined by measuring the spread of an initially sharp boundary between two solutions of different concentration in a laminar flow tube (Taylor dispersion), as described in *Rapid Commun. Mass Spectrom.* **2002,** *16*, 1454–1462. In the absence of noncovalent interactions, the measured ESI-MS dispersion profiles are expected to show a gradual transition for the macromolecule and a steep transition for the low molecular weight compound. However, if the two analytes form a noncovalent complex in solution the dispersion profiles of the two species will be very similar, since the translational diffusion of the small compound is determined by the slow Brownian motion of the macromolecule. In contrast to conventional ESI-MS-based techniques for studying noncovalent complexes, this approach does *not* rely on the preservation of solution-phase interactions in the gas phase. On the contrary, "harsh" conditions at the ion source are required to disrupt any potential gas-phase interactions between the two species, such that their dispersion profiles can be monitored separately. The viability of this technique is demonstrated in studies on noncovalent heme–protein interactions in myoglobin. Tight noncovalent binding is observed in solutions of pH 10, both in the absence and in the presence of 30% acetonitrile. In contrast, a significant disruption of the noncovalent interactions is seen at an acetonitrile content of 50%. Under these conditions, the diffusion coefficient of heme in the presence of myoglobin is only slightly lower than that of heme in a protein-free solution. A breakdown of the noncovalent interactions is also observed in aqueous solution of pH 2.4, where myoglobin is known to adopt an acid-unfolded conformation. (J Am Soc Mass Spectrom 2003, 14, 430–441) © 2003 American Society for Mass Spectrometry

Numerous physiological processes are mediated by noncovalent interactions involving biological macromolecules; examples include signaling and regulation, immune response, protein biosynthesis, and enzyme catalysis. Many drugs act by noncovalently binding to proteins or other biopolymers, often mimicking structural features of naturally occurring ligands [1]. Experimental methods capable of monitoring these interactions are of great importance. Of particular interest is the identification of high-affinity ligands for macromolecular drug targets in high-throughput screening tests of compound libraries [2, 3].

Noncovalent interactions between potential ligands and biological macromolecules can be monitored by studying the translational diffusion of these analytes in bulk solution. The diffusion coefficient D is determined by the Stokes radius R_S of a molecule according to

$$D = \frac{kT}{6\pi\eta R_s} \quad (1)$$

where k is the Boltzmann constant, T is the temperature, and η is the solution viscosity. Small molecules diffuse rapidly, whereas bigger molecules have larger Stokes radii and therefore diffuse more slowly. The binding of a small ligand to a macromolecule will significantly reduce the diffusion rate of the ligand. This idea provides the basis for measurements of noncovalent ligand–macromolecule interactions by pulsed field gradient NMR [4–11] and fluorescence correlation spectroscopy [12–14]. In a similar fashion, fluorescence polarization measurements rely on changes of the rotational diffusion coefficient upon complex formation [15]. Although these diffusion-based techniques are currently the most

Published online April 2, 2003

Address reprint requests to Dr. L. Konermann, Department of Chemistry, The University of Western Ontario, London, ON N6A 5B7, Canada. E-mail: konerman@uwo.ca

1044-0305/03/$30.00
doi:10.1016/S1044-0305(03)00123-5

Received October 29, 2002
Revised December 19, 2002
Accepted January 9, 2003

powerful tools for the high-throughput screening of combinatorial libraries [3], they are associated with a number of problems. The ability to study complex mixtures by NMR spectroscopy is limited by the difficulty of identifying unique resonances for compounds with similar structures [2]. Another difficulty is the relatively low sensitivity of NMR measurements, which often requires analyte concentrations in the millimolar range. Especially for protein solutions, nonspecific aggregation can occur under such conditions [16]. Fluorescence-based methods are far more sensitive but often require chemically labeled compounds. Other techniques, such as affinity chromatography [17] or surface plasmon resonance assays [18–21] are relatively time-consuming because they involve the chemical immobilization of compounds on solid surfaces.

Electrospray ionization mass spectrometry (ESI-MS) represents a rapid, sensitive, and highly selective alternative for monitoring noncovalent interactions [22, 23]. Most studies that use this approach rely on the ability of ESI to transfer noncovalent solution-phase assemblies into the gas phase. Numerous studies in the literature have confirmed the validity of this strategy, especially for experiments on protein–protein and protein–ligand interactions (for reviews see [24–30]). However, it is well known that the presence of noncovalent complexes in solution is *not always* correlated with the observation of the corresponding species in the mass spectrum. False-negative results are obtained when solution phase complexes dissociate prior to detection. Noncovalent binding partners that are held together primarily by hydrophobic interactions are thought to be particularly prone to dissociation during ESI, whereas electrostatic complexes are often considered to be more stable [31–33]. However, extensive dissociation during ESI is also observed for some electrostatically stabilized complexes, even under the most gentle ionization conditions [34]. ESI-MS can also produce false-positive results, i.e., some analytes tend to form noncovalent gas-phase assemblies during ESI, despite the nonexistence of the corresponding complexes in solution [35, 36]. Hu et al. have demonstrated that the nonspecific binding of metal ions to proteins can be a severe problem when the ionization conditions are not chosen properly [37]. These considerations imply that the presence or absence of noncovalent complex ions in an ESI mass spectrum does not necessarily allow conclusions to be drawn regarding specific solution phase interactions. Control experiments are often required to rule out false-positive or false-negative scenarios [24, 38, 39]. It appears that these issues are at least partly responsible for the limited acceptance of ESI-MS as a general tool for "mix and measure" experiments in the context of high-throughput screening tests [3]. The development of alternative MS-based techniques is therefore an area of great interest [40].

In this work, we present a novel ESI-MS approach for the detection of noncovalent ligand–macromolecule interactions that does *not* rely on the stability of these complexes in the gas phase. Instead, it is based on measurements of analyte diffusion in solution. The viability of this approach is explored in studies on noncovalent heme–protein interactions in myoglobin (Mb) under different solvent conditions. In native holomyoglobin (hMb) the protein adopts a largely spherical tertiary structure and forms a binding pocket into which a heme group (iron protoporphyrin IX) is noncovalently bound. Heme binding occurs through van der Waals and hydrophobic interactions, coordination of the central heme iron with His-93, and hydrogen bonds involving the two heme propionate groups [41]. Under native conditions, this noncovalent complex is extremely stable, having a dissociation constant on the order of 10^{-14} M [42]. Katta and Chait were the first to demonstrate that intact hMb can be directly observed by ESI-MS [23]. Addition of denaturants such as acid, base or organic cosolvents can induce protein unfolding and disruption of the native heme–protein interactions, thus generating apo-myoglobin (aMb) and free heme. The solution-phase transitions from hMb to aMb and vice versa have been extensively studied, both optically [43–45] and by ESI-MS [29, 39, 46–51]. The results of this work demonstrate that diffusion measurements by ESI-MS are a sensitive method for probing noncovalent heme–protein interactions in solution.

Experimental

Chemicals

Horse skeletal muscle ferri-myoglobin, equine hemin chloride, and piperidine were purchased from Sigma (St. Louis, MO). Glass-distilled acetonitrile was obtained from Caledon Laboratories Ltd. (Georgetown, ON). Glacial acetic acid and HPLC-grade methanol were products of Fisher Scientific (Nepean, ON). All chemicals were used without further purification. Solutions were prepared in freshly distilled water prepurified by reverse osmosis. Solution pH values were measured using an accumet pH meter (Fisher Scientific). Piperidine and acetic acid were used to adjust the pH of basic and acidic solutions, respectively. Percent compositions are reported on a volume/volume basis. All protein solutions were prepared by using lyophilized hMb, thus automatically ensuring a molar heme:protein ratio of 1:1.

Optical Spectroscopy and ESI-MS

Absorption spectra of 5 μM Mb solutions were recorded on a Cary 100 spectrophotometer (Varian, Mississauga, ON). Fluorescence emission spectra of 5 μM Mb solutions were measured on a Spex Fluorolog 3 fluorimeter (Instruments S.A., Edison, NJ) using an excitation wavelength of 280 nm. The reported fluorescence intensities correspond to those measured at an emission wavelength of 342 nm. Circular dichroism (CD) spectra were recorded on a Jasco J-810 spectropolarimeter (Eas-

ton, MD) using a 0.1 cm path length cuvette. For the wavelength range between 190 and 250 nm, 15 μM myoglobin solutions were used, for the range between 250 and 320 nm the protein concentration was increased to 50 μM. ESI mass spectra of Mb at pH 10 were recorded on an API 365 triple quadrupole mass spectrometer (Sciex, Concord, ON) using "soft" ionization conditions (orifice potential = 10 V, ring potential = 120 V, skimmer potential = 0 V), at a liquid flow rate of 5 μL/min and a protein concentration of 10 μM. For all MS experiments described in this study, ions were generated by pneumatically-assisted ESI ("ion spray") in the positive ion mode. Deconvoluted mass distributions were generated by using the software package BioMultiView (Sciex, Concord, ON).

Diffusion Measurements

Dispersion profiles were recorded as described [52]. Briefly, a syringe connected to an inlet tube is employed to fill the laminar flow tube with solution containing of 5 μM analyte (Mb or heme). A sliding block mechanism is then used to push the inlet tube out of alignment with the laminar flow tube, such that the inlet tube can be filled with 10 μM analyte solution without disturbing the contents of the flow tube. Upon realigning the tubes, a sharp boundary is created between the two solutions at the start of the flow tube. At time $t = 0$, a syringe pump (Harvard Apparatus, South Nattick, MA) starts delivering 10 μM analyte solution into the flow tube at a flow rate of 5 μL/min. The addition of 5 μM analyte to the initial solvent in the flow tube is a precautionary measure to prevent possible artifacts due to wall adsorption processes.

The laminar flow tube used consists of Teflon and has an i.d. of 258.2 μm (Upchurch, Oak Harbor, WA). Slightly different flow tube lengths around 3 m were used for individual experiments. After passing through the flow tube, the solution is mixed with a makeup solvent at 5 μL/min for a total flow rate of 10 μL/min at the ion source. Different solvent systems were employed to optimize the signal stability for each set of conditions. Acetonitrile-containing analyte solutions were mixed with a solvent composed of 50% water, 30% acetonitrile, and 20% acetic acid. For aqueous solutions at pH 10, a makeup solvent of 80% methanol and 20% acetic acid was used; for myoglobin in water at pH 2.4, the makeup solvent composition was 95% methanol and 5% acetic acid. Dispersion profiles were generated by recording the intensities of heme$^+$ (*m/z* 616.2) and aMb^{17+} (*m/z* 998.2) as a function of time. This was done by selected ion monitoring on a Sciex "Toby" single-quadrupole mass spectrometer (orifice-skimmer potential difference = 100 V). Diffusion coefficients of heme and protein were determined by fitting the measured dispersion profiles based on the theoretical expression given in eq 17 of reference [52]. Each reported diffusion coefficient represents an average of around ten independent measurements, errors correspond to one standard deviation. Solution viscosities had to be determined for the calculation of Stokes radii. These measurements were performed by using a Cannon-Ubelholde capillary viscometer (VWR Canlab, Mississauga, ON) which allows viscosities to be determined with an error of less than 2%. For aqueous solutions of pH 10 in the presence of 0, 30, and 50% acetonitrile, the viscosities were determined to be 8.97×10^{-4} kg m^{-1} s^{-1}, 9.53×10^{-4} kg m^{-1} s^{-1}, and 8.29×10^{-4} kg m^{-1} s^{-1}, respectively. For an aqueous solution of 5% acetic acid a viscosity of 9.79×10^{-4} kg m^{-1} s^{-1} was measured. The viscosity changes observed upon addition of 10 μM Mb or heme to these solutions were insignificant. All experiments were carried out at room temperature (22 $\pm$ 1° C).

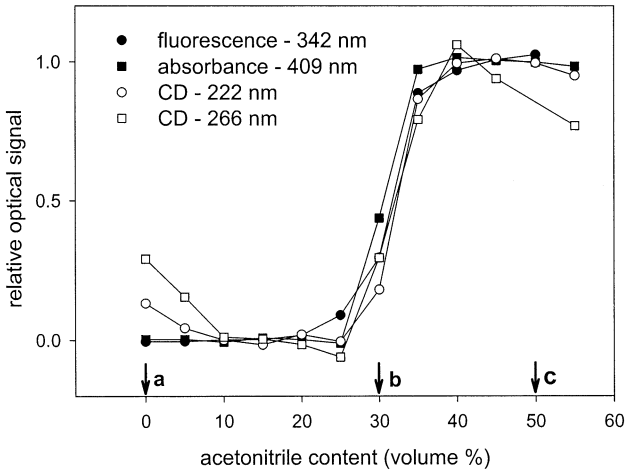

Figure 1. Acetonitrile-induced denaturation of myoglobin at pH 10 monitored by optical spectroscopy. Arrows labeled a, b, c indicate the solvent conditions used in subsequent ESI-MS experiments. Filled circles: Tryptophan fluorescence monitored at 342 nm; filled squares: heme absorption monitored at 409 nm; open circles: ellipticity at 222 nm, measured by circular dichroism spectroscopy; open squares: ellipticity at 266 nm. All four curves have been normalized to unity.

Results and Discussion

Optical Studies and ESI Mass Spectra

In an initial set of experiments, the effects of acetonitrile on the Mb structure and on the noncovalent heme–protein interactions were studied by optical spectroscopy (Figure 1). Because the solubility of free heme at acidic and near-neutral pH is very limited, these studies were carried out at pH 10. The same pH was used for the ESI-MS experiments described below. In the absence of organic cosolvents, the protein adopts a tightly folded structure at pH 10, with the heme group seated in the binding pocket (see [39, 51] and references therein).

Circular dichroism (CD) spectroscopy was used to monitor changes of the polypeptide structure. The CD signal measured at 222 nm, which is indicative of the α-helical content [53–55], changed from -15.1×10^3 deg

$cm^2\ dmol^{-1}$ in the absence of acetonitrile to -9.77×10^3 deg $cm^2\ dmol^{-1}$ in 55% acetonitrile, with a sharp transition centered around 33% acetonitrile. These data show that acetonitrile induces a substantial collapse of the Mb helical structure. A similar transition was seen in the near-UV region at 266 nm, where the ellipticity changed from 0.38×10^3 deg $cm^2\ dmol^{-1}$ to 0.31×10^3 deg $cm^2\ dmol^{-1}$, thus indicating a significant breakdown of the protein's tertiary structure [56, 57]. The solvent accessibility of the heme group can be probed by absorbance changes in the wavelength range around 400 nm (Soret region). A marked decrease in the absorption at 409 nm indicates that the heme group becomes exposed to the solvent upon unfolding at high acetonitrile concentrations [58–62]. Also, measurements of the tryptophan fluorescence provide a sensitive probe for monitoring heme–protein interactions in Mb. In native Mb, the fluorescence from Trp14 and, to a lesser degree, from Trp7 is quenched because of resonance energy transfer to the heme group [61–63]. The drastic increase of the relative Trp fluorescence intensity observed at high acetonitrile concentrations suggests that denaturation is accompanied by a substantial increase of the heme-tryptophan distances.

In summary, the optical data depicted in Figure 1 show that the addition of acetonitrile to hMb at pH 10 induces protein unfolding, and leads to a significant disruption of the heme–protein interactions. All four optical probes show similar unfolding curves, with midpoints around an acetonitrile content of 33%. This suggests that the denaturation of Mb under these conditions is a cooperative (two-state) process. However, the occurrence of folding intermediates or intermediate modes of heme binding cannot be totally ruled out [64]. It seems possible that even at high acetonitrile concentrations some residual heme–protein interactions persist [62]. Evidence for interactions of this kind in denatured Mb has previously been obtained by vibrational spectroscopy, albeit under different solvent conditions [65]. The ESI-MS data presented below indicate that weakly associated complexes between unfolded Mb and heme may also persist under the conditions of the current study.

The three arrows in Figure 1 mark the acetonitrile concentrations that were used in subsequent ESI-MS experiments; they are (1) 0% acetonitrile, corresponding to native (or native-like) myoglobin with the heme group firmly attached, (2) 30% acetonitrile, corresponding to the onset of denaturation, and (3) 50% acetonitrile, corresponding to unfolded myoglobin, under conditions where the native heme–protein interactions are significantly disrupted. ESI mass spectra corresponding to these solvent conditions are depicted in Figure 2. The orifice-skimmer potential difference in the ion sampling interface of the mass spectrometer was chosen as low as possible for these experiments (see the Experimental section), to minimize possible fragmentation of the heme–protein complex in the gas phase [48, 66]. As expected, the spectrum shown in Figure 2a (0% acetonitrile) exclusively shows hMb ions in relatively low charge states (around hMb^{10+}), which is consistent with the tightly folded conformation of the intact heme–protein complex in solution [23, 39, 46, 47, 49–51]. The deconvoluted mass distribution obtained from this spectrum shows a maximum at 17564 Da, which is in good agreement with the mass expected for the intact heme–protein complex (17568 Da). The spectrum depicted in Figure 2b (30% acetonitrile) shows a mixture of hMb and aMb ions, the latter ones being the predominant species. This spectrum is shifted to slightly higher charge states and shows aMb^{11+} as the most abundant ion. Close inspection reveals the presence of a third species, which corresponds to Mb with two heme groups attached. Previous studies strongly suggest that these ions reflect the presence of solution-phase proteins that are bound to heme dimers [39, 51]. The deconvoluted mass distribution in Figure 2b shows three major peaks, corresponding to aMb (16950 Da), hMb, and Mb with two heme groups (18181 Da). The masses measured for aMb and for the two-heme species are in good agreement with the expected values of 16952 Da and 18184 Da, respectively.

Surprisingly, the ESI mass spectrum of Mb recorded in the presence of 50% acetonitrile (Figure 2c) looks very similar to that obtained at 30% acetonitrile. Based on the optical data discussed above, the contribution of aMb ions would be expected to be much higher at 50% acetonitrile. The significant changes in the nature of the heme–protein interactions, taking place between 30 and 50% acetonitrile, are not reflected in the ESI mass spectra. Qualitatively similar observations have been reported previously, e.g., for acyl CoA binding protein, where complexes representing vastly different solution-phase binding affinities resulted in virtually the same ESI mass spectra [31]. The reasons underlying this lack of correlation between solution-phase and gas-phase abundance are not clear. In the present case, this effect could be rationalized by assuming different relative ionization efficiencies of solution-phase hMb and aMb for the different solvent conditions used. However, without further experimental evidence this explanation remains speculative.

Diffusion Studies

We previously introduced a method for measuring analyte diffusion coefficients by ESI-MS [52]. ESI-MS is used to monitor the Taylor dispersion of an initially sharp boundary between two analyte solutions of different concentration in a laminar flow tube [67–72]. Under laminar flow conditions, the velocity profile in a circular tube is given by

$$v(r) = v_{max}\left(1 - \frac{r^2}{R^2}\right) \quad (2)$$

where R and r are the inner radius and distance from

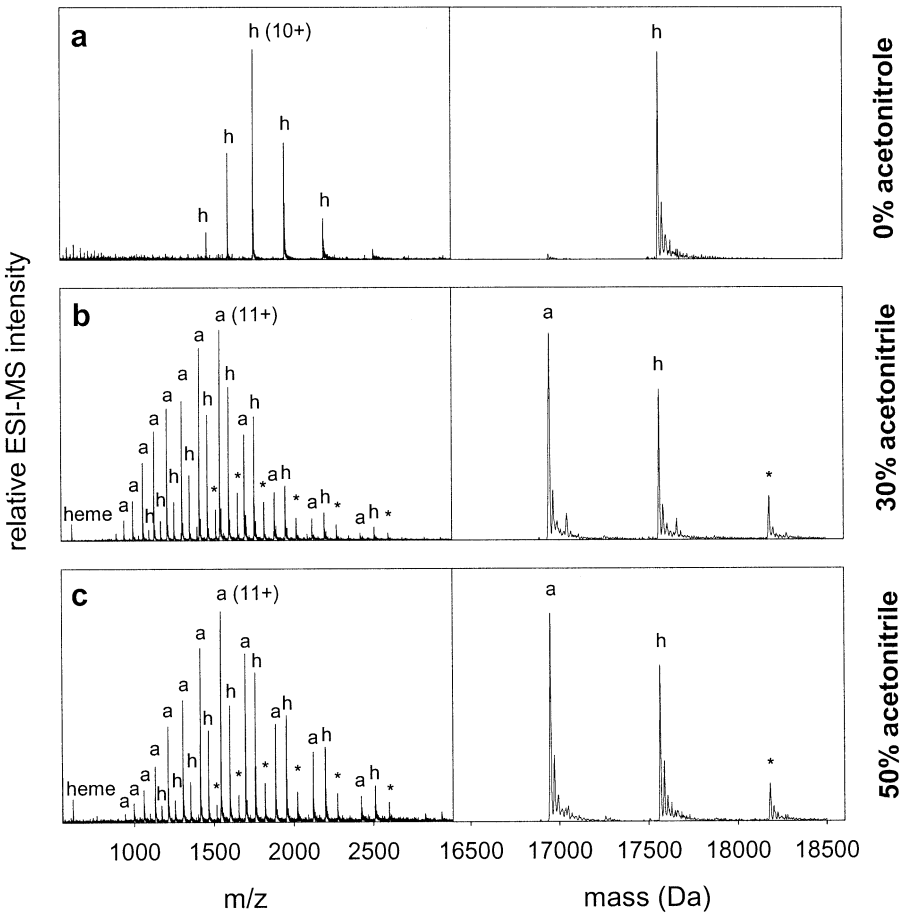

Figure 2. ESI mass spectra (left hand side panels) of myoglobin recorded at pH 10 in (**a**) aqueous solution (0% acetonitrile); (**b**) 30% acetonitrile; (**c**) 50% acetonitrile. Notation: a, apomyoglobin (protein ions without heme group); h, holomyoglobin (protein ions with heme group attached). Peaks labeled with asterisks correspond to myoglobin with two heme groups attached. Also indicated are the charge states of selected ions. Deconvoluted mass distributions are shown in the panels on the right hand side.

the center of the tube, respectively. Liquid at the centerline ($r = 0$) moves with the maximum velocity v_{max}, which is twice the average flow velocity v, while the liquid at the tube wall ($r = R$) is stationary. Diffusion experiments are carried out by initially filling a flow tube of length l with dilute analyte solution. One end of the tube is connected to the ESI source of the mass spectrometer, whereas the other end is connected to a reservoir of more concentrated analyte solution. At time $t = 0$, a pump starts delivering this more concentrated solution into the flow tube, and the ESI mass spectrometer starts monitoring the "dispersion profile", i.e., the signal intensity as a function of time. The profile expected based on eq 2 is depicted in Figure 3a. It shows a low signal intensity, until the more concentrated solution starts reaching the end of the tube at $t = l/v_{max}$. Subsequently, the intensity increases asymptotically to a maximum value. This scenario does not take into account analyte diffusion which constantly changes the radial position of individual molecules and causes them to exchange between zones of higher and lower flow velocity, thus counteracting the dispersion caused by the laminar velocity profile. If this exchange is rapid (i.e., for large values of D), all molecules tend to travel with roughly the same average velocity $v = v_{max}/2$, thus leading to a dispersion profile that shows a steep transition around $t = 1/v$. For smaller values of D, this averaging effect is less pronounced, and therefore the corresponding transitions will not be as steep. Under typical operating conditions, only radial diffusion has to be taken into account, i.e., the contribution of diffusion along the tube is completely negligible [52, 67].

Now we will consider the case where the analyte solution represents a mixture of a macromolecular species and a low molecular weight compound. For reasons of simplicity it is assumed that the concentrations of the two analytes are identical. In the absence of noncovalent solution-phase interactions, the diffusion of the two solutes is independent. Therefore, a steep dispersion profile will be seen for the small molecule, whereas the macromolecule will exhibit a more gradual transition (Figure 3b). However, if the two analytes form a noncovalent complex, the diffusion behavior of both species will be determined by the slow Brownian

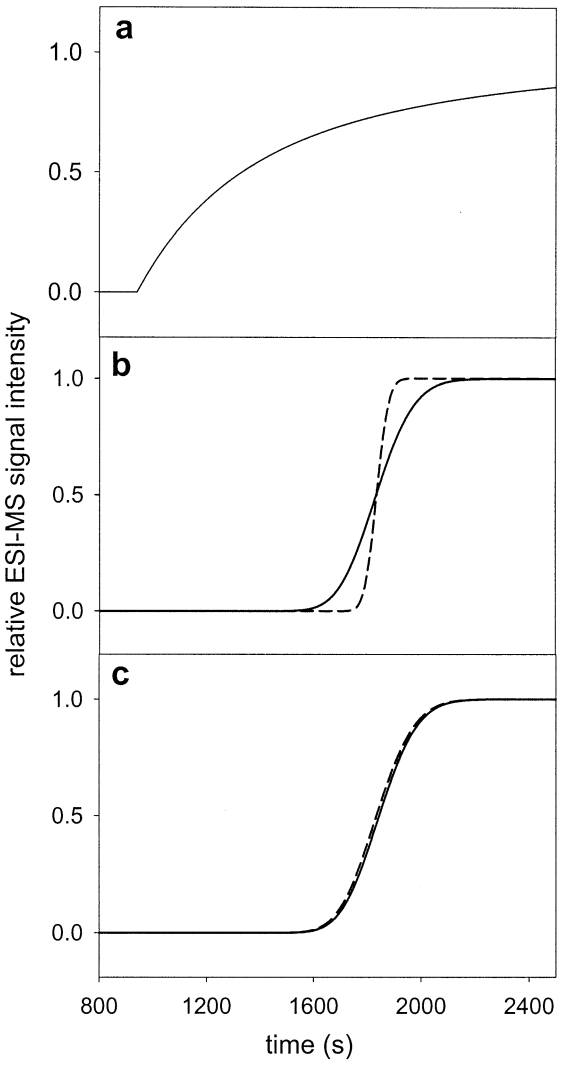

Figure 3. Simulated ESI-MS dispersion profiles, representing the signal intensity of selected analytes at the end of a laminar flow tube under different conditions. (**a**) Dispersion profile expected for a single analyte in the absence of diffusion, i.e., $D = 0$. (**b**) Dispersion profiles expected for a macromolecule ($D = 1 \times 10^{-10}$ m^2/s, solid curve), and a small molecule ($D = 10 \times 10^{-10}$ m^2/s, dashed curve). It is assumed that the two analytes do *not* interact in solution. (**c**) Dispersion profiles as in (**b**), but under the assumption of tight noncovalent binding between the two analytes. Under these conditions the profiles measured for the two species will be identical (for the purpose of presentation, one of the profiles has been slightly shifted). Parameters used: Tube length $l = 3$ m, tube radius $R = 129.1$ μm, flow rate = 5 μL/min (corresponding to $v_{max} = 3.18 \times 10^{-3}$ m/s). The dispersion profile in panel (**a**) has been calculated based on eq 19 in reference [52], all the other profiles have been calculated based on eq 17 from the same reference. For simplicity, all dispersion profiles have been normalized to unity. Further explanations are given in the text.

motion of the macromolecule. In other words, *noncovalent binding will drastically change the dispersion profile of the small molecule*. A tightly bound ligand will exhibit the same profile as the macromolecule (Figure 3c). This experimental strategy requires the conditions at the ion source to be harsh enough to ensure that noncovalent binding does not persist in the gas phase, such that both species can be monitored individually.

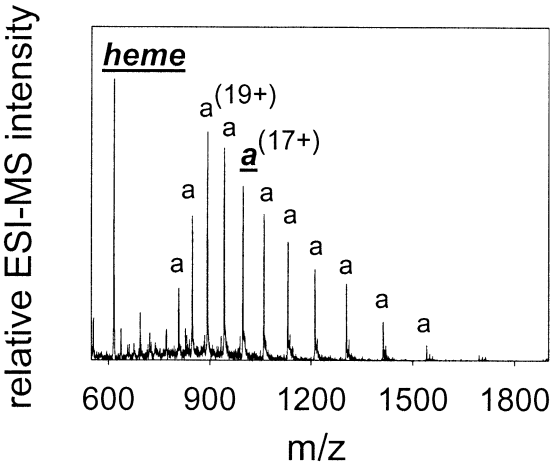

Figure 4. ESI mass spectrum of myoglobin recorded after addition of a makeup solvent to the protein solution in the laminar flow tube (see text). Solution conditions at the source: 30% acetonitrile, 10% acetic acid, pH 2.4 (the initial pH before mixing was 10.0). For notation see the caption of Figure 3. Intensities of ions marked bold and underlined, corresponding to $heme^+$ and $[aMb + 17H]^{17+}$, were monitored in subsequent diffusion experiments. Note that the *x*-axis in this figure is scaled differently from that in Figure 3.

To assess the viability of the described diffusion approach we studied the noncovalent heme–protein interactions in myoglobin under the conditions used above, i.e., in aqueous solutions of different acetonitrile content at pH 10. For measuring ESI-MS dispersion profiles, all Mb solutions were mixed with an acetic acid-containing makeup solvent after passing through the laminar flow tube. In all cases, the final pH after mixing was around 2.4, which induces protein unfolding and the disruption of the solution-phase heme–Mb interactions [50, 73]. To promote the dissociation of possible residual hMb ions in the gas phase, relatively harsh voltage settings were used in the ion sampling interface of the mass spectrometer (see the Experimental section). Mass spectra recorded under these conditions are dominated by highly charged aMb ions, regardless of the solvent environment in the flow tube (Figure 4). The spectra show aMb ions in high charge states, with a maximum around aMb^{19+} which is typical for acid-unfolded Mb [23, 39, 46, 47, 49–51] (Figure 4). In addition, a strong signal due to free heme is observed. We attribute the relatively noisy baseline of spectra recorded under these conditions to the substantial salt content of the solutions, which had been acidified from 10 to 2.4 pH. A number of minor peaks observed at low *m/z* may correspond to protein fragments that were generated by collision-induced dissociation.

Dispersion profiles of heme and protein were generated by monitoring the intensities of $heme^+$ and aMb^{17+} as a function of time. Diffusion coefficients were determined from the measured profiles as described in the Experimental section [52]. For each of the three acetonitrile concentrations, control experiments were carried

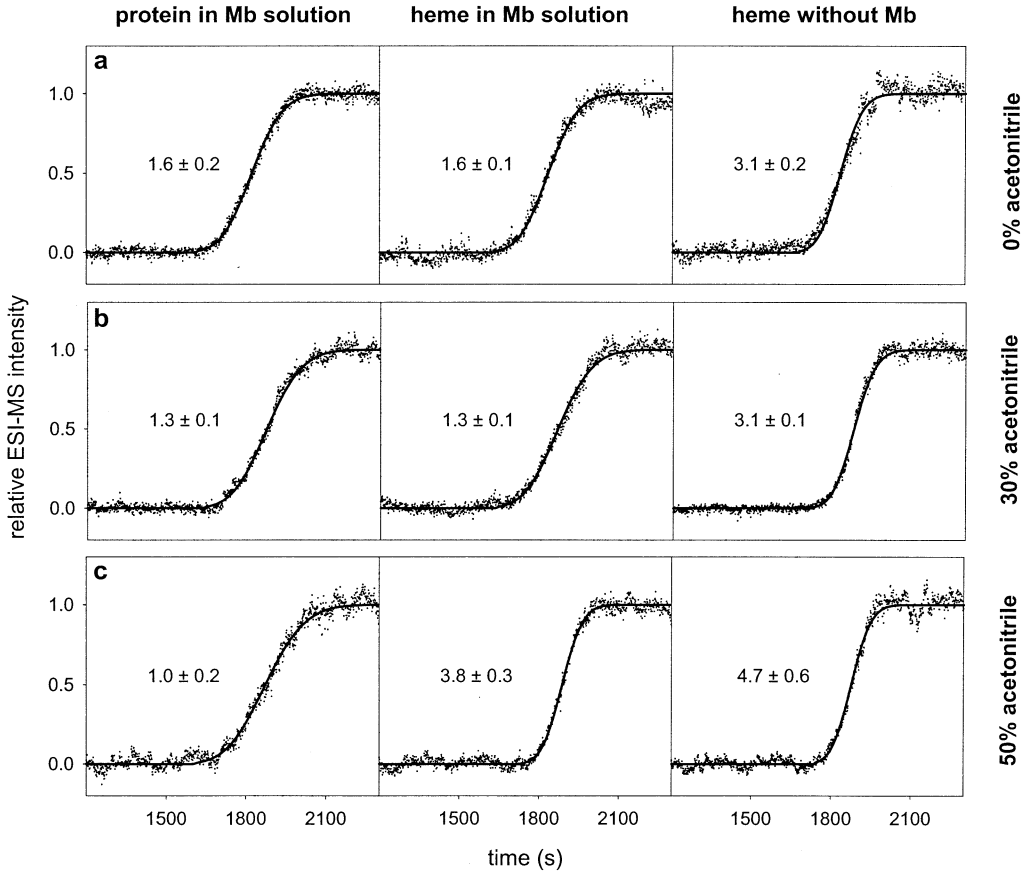

Figure 5. ESI-MS dispersion profiles recorded for protein (first column) and heme (second column) in solutions of myoglobin at pH 10. The third column shows dispersion profiles recorded for heme in protein-free solutions. The experiments were carried out in the presence of (**a**) 0% acetonitrile, (**b**) 30% acetonitrile, and (**c**) 50% acetonitrile. Solid lines are fits to the experimental data according to eq 17 in reference [52]. The diffusion coefficients determined from these fits, in units of 10^{-10} m^2 s^{-1}, are indicated in each panel.

out to determine the diffusion coefficient of heme in the absence of Mb. Readers are reminded that the steepness of the measured dispersion profile increases with increasing D. Figure 5a shows profiles recorded for flow tube conditions of pH 10 and 0% acetonitrile. Protein and heme show virtually the same profiles with diffusion coefficients of (1.6 ± 0.2) × 10^{-10} m^2 s^{-1} and (1.6 ± 0.1) × 10^{-10} m^2 s^{-1}, respectively. This finding is consistent with the known tight noncovalent heme–protein interactions under these solvent conditions. A significantly higher diffusion coefficient of (3.1 ± 0.2) × 10^{-10} m^2 s^{-1} was measured for heme in the absence of Mb, thus confirming that noncovalent binding to the protein does indeed reduce the heme diffusion rate.

The addition of 30% acetonitrile to the solution slightly decreases the diffusion coefficient of the protein to (1.3 ± 0.1) × 10^{-10} m^2 s^{-1} (Figure 5b). Within experimental error, this is identical to the diffusion coefficient measured for heme in the Mb solution, which shows that heme and protein remain noncovalently associated under these conditions. Again, a significantly higher value of D, (3.1 ± 0.1) × 10^{-10} m^2 s^{-1}, was measured for heme in a protein-free solution.

In contrast, the dispersion profiles recorded in the presence of 50% acetonitrile point to a significant decrease in the strength of the noncovalent heme–protein interactions (Figure 5c). Under these conditions, heme in Mb solution shows a diffusion coefficient of (3.8 ± 0.3) × 10^{-10} m^2 s^{-1}, which is substantially higher than the value of (1.0 ± 0.2) × 10^{-10} m^2 s^{-1} measured for the protein. However, the diffusion coefficient of heme in the Mb solution is still somewhat lower than the value of (4.7 ± 0.6) × 10^{-10} m^2 s^{-1} that was found in the absence of protein. Taken together, these findings suggest that the heme–protein interactions in 50% acetonitrile are significantly disrupted, but that some residual binding may persist. The latter is in line with the observation of hMb ions in the ESI mass spectrum of Mb recorded under these solvent conditions (Figure 2c).

Diffusion measurements on Mb were also carried out by using an aqueous solution of 5% acetic acid (pH 2.4) as flow tube solvent. At this pH, the protein is known to adopt an extensively unfolded conformation in solution [16]. ESI mass spectra recorded under these conditions closely resemble that depicted in Figure 4, with aMb^{19+} as the most intense protein ion (data not shown). From

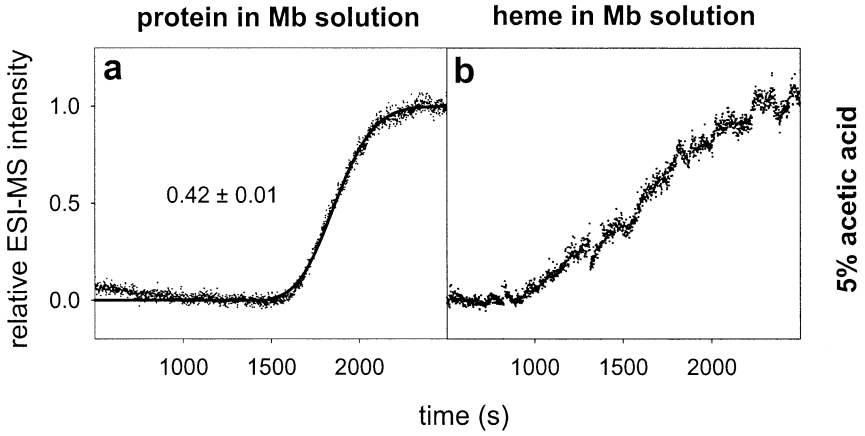

Figure 6. ESI-MS dispersion profiles recorded for protein (**a**) and heme (**b**) in a solution of myoglobin at pH 2.4. Note the different time scale compared to Figure 5. For further explanation see text, and the caption of Figure 5.

the measured dispersion profiles, the diffusion coefficient of the protein was determined to be (0.42 ± 0.01) $\times 10^{-10}$ m^2 s^{-1} (Figure 6a). This value is lower than for any other solvent condition used in this work. The dispersion profiles of the heme group (Figure 6b) could not be described by the sigmoidal model function that was used for the other profiles. As a consequence, the diffusion coefficient of heme could not be determined in this experiment. Qualitatively, the heme dispersion profile resembles that shown in Figure 3a, which was calculated based on the assumption of no diffusion at all (note the signal onset around $t = l/v_{max} \approx 940$ s, in Figures 3a and 6b). We ascribe this effect to the known tendency of heme to undergo extensive aggregation at acidic pH (see [39, 51] and references therein). Presumably, the Stokes radii of these aggregates are large enough to substantially suppress diffusion on the experimental time scale of ~2500 s. The observation of a totally different diffusion behavior for heme and protein clearly indicates that noncovalent interactions between the two species are extremely weak or nonexistent for these acidic conditions. This reflects the fact that tight heme–protein interactions in Mb require the binding pocket to be in a native-like conformation, a condition that is not met for the acid-denatured protein at pH 2.4 [16]. Unfortunately, the limited heme solubility at acidic pH precluded diffusion measurements in the absence of protein in this set of experiments.

Stokes Radii

Based on the measured diffusion coefficients, the Stokes radii R_S of heme and protein can be calculated from eq 1 for the various flow tube solvent conditions used (Figure 7). The R_S values allow a direct comparison of analyte "size", without being obscured by the different solvent viscosities of the individual experiments [74]. In solutions of 0 and 30% acetonitrile content at pH 10, the R_S values of heme in Mb solution are close to those of the protein, which reflects the fact that the two species form a stable noncovalent complex. In contrast, heme in Mb solution and in the presence of 50% acetonitrile has a Stokes radius close to that measured in a protein-free environment, thus indicating the disruption of the noncovalent heme–protein interactions. The Stokes radius of (1.6 ± 0.2) nm that was measured for tightly folded hMb is slightly lower than the value of 2.2 nm that has previously been determined for the native apoprotein by size-exclusion chromatography [75]. This is consistent with the fact that hMb under native conditions has a more compact conformation than aMb [16, 76]. Addition of 50% acetonitrile moderately increases the R_S value of the protein to (2.6 ± 0.4) nm, thus indicating a somewhat more expanded conformation. A dramatic increase to (5.2 ± 0.1) nm is seen at pH 2.4, where Mb is known to be extensively unfolded [16].

It is interesting to consider the relationship between the R_S values measured for the protein, and the ESI mass spectra recorded under the corresponding solvent conditions. The addition of acetonitrile to Mb solutions at pH 10 induces a slight shift of the mass spectrum to higher charge states (Figure 2). In contrast, a more dramatic shift is seen in the spectrum of the acid-unfolded protein at pH 2.4 (data not shown; the observed charge state distribution is virtually identical to that depicted in Figure 4). These observations are in line with the well known fact that the ESI charge state distribution represents a sensitive probe of protein conformational changes. It is generally accepted that protein unfolding in solution leads to the formation of more highly charged protein ions in positive-ion ESI [77–83]. However, the physical basis of this phenomenon is still a matter of debate [23, 84, 85]. According to one hypothesis, a major determinant of the ESI charge state distribution is the "compactness" of a protein in solution [51, 83, 86–88]. This notion is compatible with the data presented here. The Stokes radius is a measure of the volume occupied by a protein [74], and there is a qualitative correlation between the measured R_S values,

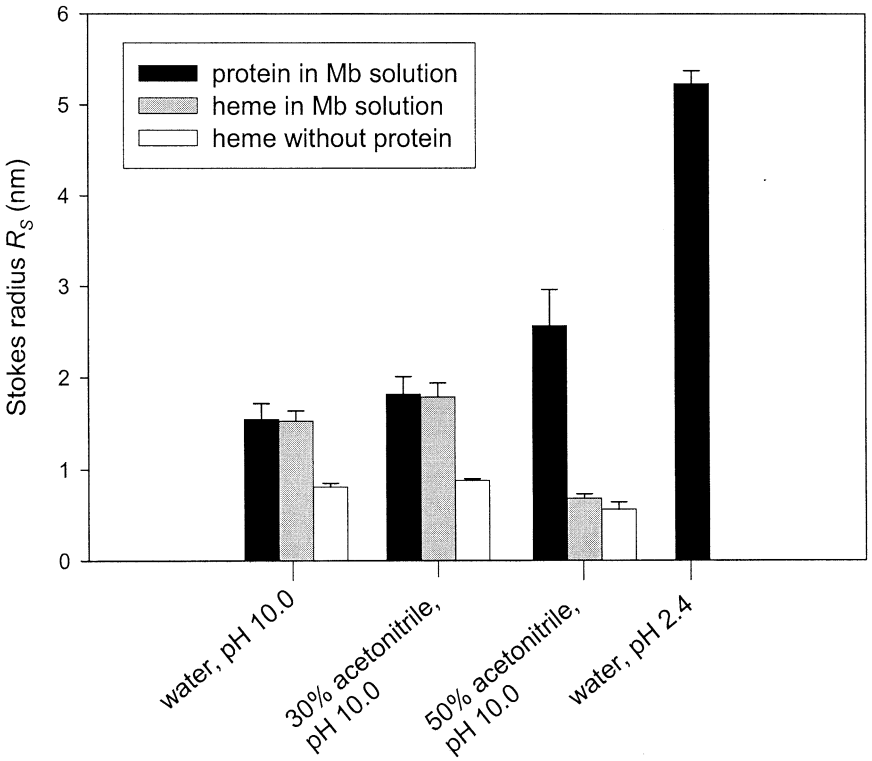

Figure 7. Stokes radii R_S of myoglobin and heme, calculated from eq 1 based on the diffusion coefficients given in Figures 5 and 6 for the solution conditions indicated. Problems with heme solubility precluded the determination of heme R_S values at pH 2.4 (see text).

and the corresponding shifts seen in the ESI charge state distribution of the protein.

When comparing the Stokes radii of heme measured in protein-free solution, it is noted that a somewhat lower R_S value is observed in 50% acetonitrile compared to experiments that were carried out with 0 and 30% acetonitrile. Heme is moderately soluble under all of these conditions. However, it probably is not a monomeric species in solution but instead forms small aggregates consisting of a few molecules. Owing to its hydrophobicity, the solubility of heme is epected to increase as the percentage of acetonitrile in solution is raised, thus decreasing the average aggregate size [89]. This effect could provide an explanation for the trend in the measured heme Stokes radii.

Conclusions

In this work we have presented a novel ESI-MS-based technique for monitoring noncovalent ligand–macromolecule interactions in solution. Our approach does not rely on the preservation of noncovalent complexes in the gas phase, instead it is based on measurements of analyte diffusion behavior in solution. When a small ligand noncovalently binds to a macromolecule, both analytes will essentially show the same diffusion behavior, which will be determined by the slow Brownian motion of the larger species. For these diffusion studies, any existing complexes are deliberately disrupted immediately prior to ESI, in order to allow the independent measurement of both signal intensities. This can be achieved through a combination of "harsh" declustering voltages in the ion sampling interface of the mass spectrometer, and through the addition of denaturing "ESI friendly" co-solvents, such as volatile acids and organic liquids. As a convenient side-effect, this measure will often improve the signal intensity and stability, especially in cases where aqueous solutions of near-neutral pH are used in the flow tube. In the present case, this technique was applied to study heme–protein interactions in Mb under different solvent conditions. Optical spectroscopy clearly indicates significant changes in the nature of the noncovalent interactions between 30 and 50% acetonitrile content. Surprisingly, ESI mass spectra recorded under these conditions have essentially the same appearance. In contrast, the breakdown of the heme–protein interactions is clearly apparent in the measured ESI-MS dispersion profiles.

To minimize the time and the amount of sample required for the approach presented in this work, it will be necessary to reduce the dimensions of the laminar flow tube; possibly this could be done by using microfluidic chip technology [90]. The applicability of ESI-MS-based diffusion measurements as a tool for high-throughput binding assays remains to be evaluated. As a first step in this direction, we are currently testing the viability of this approach in experiments

involving receptor proteins in the presence of multiple potential ligands representing different binding affinities.

Acknowledgments

The authors gratefully acknowledge helpful discussions with Derek Leaist and Nils Petersen. They also thank David Magri and Mark S. Workentin for their help with the SPEX fluorimeter. CD experiments were carried out with the help of Yumin Bi and Stanley D. Dunn at the UWO Biomolecular Interactions and Conformation Facility, which is supported by a multi-user equipment and maintenance grant from the Canadian Institutes of Health Research. This work was financially supported by the Natural Sciences and Engineering Research Council of Canada and by The University of Western Ontario.

References

1. George, S. R.; O'Dowd, B. F.; Lee, S. P. G-Protein-Coupled Receptor Oligomerization and its Potential for Drug Discovery. *Nat. Rev. Drug Discov.* **2002,** *1,* 808–820.
2. Hajduk, P.; Meadows, R. P.; Fesik, S. W. NMR-Based Screening in Drug Discovery. *Q. Rev. Biophys.* **1999,** *32,* 211–240.
3. Wölcke, J.; Ullmann, D. Miniaturized HTS Techologies—uHTS. *Drug Discov. Today* **2001,** *6,* 637–646.
4. Gounarides, J. S.; Chen, A.; Shapiro, M. J. Nuclear Magnetic Resonance Chromatography: Applications of Pulse Field Gradient Diffusion NMR to Mixture Analysis and Ligand–Receptor Interactions. *J. Chromatogr. B* **1999,** *725,* 79–90.
5. Lin, M.; Shapiro, M. J.; Wareing, J. R. Diffusion-Edited NMR-Affinity NMR for Direct Observation of Molecular Interactions. *J. Am. Chem. Soc.* **1997,** *119,* 5249–5250.
6. Bleicher, K.; Lin, M.; Shapiro, M. J.; Wareing, J. R. Diffusion Edited NMR: Screening Compound Mixtures by Affinity NMR to Detect Binding Lignads to Vancomycin. *J. Org. Chem.* **1998,** *63,* 8486–8490.
7. Morris, K. F.; Stilbs, P.; Johnson, C. S. Analysis of Mixtures Based on Molecular Size and Hydrophobicity by Means of Diffusion-Ordered 2D NMR. *Anal. Chem.* **1994,** *66,* 211–215.
8. Buevich, A. V.; Baum, J. Residue-Specific Real-Time NMR Diffusion Experiments Define the Association States of Proteins During Folding. *J. Am. Chem. Soc.* **2002,** *124,* 7156–7162.
9. Anderson, R. C.; Lin, M.; Shapiro, M. J. Affinity NMR: Decoding DNA Binding. *J. Comb. Chem.* **1999,** *1,* 69–72.
10. Lin, M.; Larive, C. K. Detection of Insulin Aggregates with Pulsed-Field Gradient Nuclear Magnetic Resonance Spectroscopy. *Anal. Biochem.* **1995,** *229,* 214–220.
11. Hodge, P.; Monvisade, P.; Morris, G. A.; Preece, I. A Novel NMR Method for Screening Soluble Compound Libraries. *Chem. Commun.* **2001,** *3,* 239–240.
12. Rigler, R. Fluorescence Correlations, Single Molecule Detection and Large Number Screening. Applications in Biotechnology. *J. Biotech.* **1995,** *41,* 177–186.
13. Gradl, G.; Guenther, R.; Sterrer, S. Fluorescence Correlation Spectroscopy (FCS): Measuring Biological Interactions in Microstructures. *BioMethods* **1999,** *10,* 331–351.
14. Auer, M.; Moore, K. J.; Meyer-Almes, F. J.; Guenther, R.; Pope, A. J.; Stoeckli, K. A. Fluorescence Correlation Spectroscopy: Lead Discovery by Miniaturized HTS. *Drug Discov. Today* **1998,** *3,* 457–565.
15. Rogers, M. V. Light on High-Throughput Screening: Fluorescence-Based Assay Technologies. *Drug Discov. Today* **1997,** *2,* 156–160.
16. Hughson, F. M.; Wright, P. E.; Baldwin, R. L. Structural Characterization of a Partly Folded Apomyoglobin Intermediate. *Science* **1990,** *249,* 1544–1548.
17. Fassina, G. Affinity Chromatography. In *Encyclopedia of Life Sciences (www.els.net)*; Nature Publishing Group: London, 2001.
18. Myszka, D. G.; Rich, R. L. Implementing Surface Plasmon Resonance Biosensors in Drug Discovery. *Pharm. Sci. Tech. Today* **2000,** *3,* 310–317.
19. McDonnell, J. M. Surface Plasmon Resonance: Towards an Understanding of the Mechanisms of Biological Molecular Recognition. *Curr. Opin. Chem. Biol.* **2001,** *5,* 572–577.
20. Chu, Y.-H.; Dunayevskiy, Y. M.; Kirby, D. P.; Vouros, P.; Karger, B. L. Affinity Capillary Electrophoreses-Mass Spectrometry for Screening Combinatorial Libraries. *J. Am. Chem. Soc.* **1996,** *118,* 7827–7835.
21. Natsume, T.; Nakayama, H.; Jansson, O.; Isobe, T.; Takio, K.; Mikoshiba, K. Combination of Biomolecular Interaction Analysis and Mass Spectrometric Amino Acid Sequencing. *Anal. Chem.* **2000,** *72,* 4193–4198.
22. Ganem, B.; Li, Y.-T.; Henion, J. D. Observation of Noncovalent Enzyme–Substrate and Enzyme–Product Complexes by Ion Spray Mass Spectrometry. *J. Am. Chem. Soc.* **1991,** *113,* 7818–7819.
23. Katta, V.; Chait, B. T. Observation of the Heme–Globin Complex in Native Myoglobin by Electrospray-Ionization Mass Spectrometry. *J. Am. Chem. Soc.* **1991,** *113,* 8534–8535.
24. Smith, D. L.; Zhang, Z. Probing Noncovalent Structural Features of Proteins by Mass Spectrometry. *Mass Spectrom. Rev.* **1994,** *13,* 411–429.
25. Winston, R. L.; Fitzgerald, M. C. Mass Spectrometry as a Readout of Protein Structure and Function. *Mass Spectrom. Rev.* **1997,** *16,* 165–179.
26. Hernandez, H.; Robinson, C. V. Dynamic Protein Complexes: Insights from Mass Spectrometry. *J. Biol. Chem.* **2001,** *276,* 46685–46688.
27. Rostom, A. A.; Robinson, C. V. Disassembly of Intact Multiprotein Complexes in the Gas Phase. *Curr. Opin. Struct. Biol.* **1999,** *9,* 135–141.
28. Loo, J. A. Studying Noncovalent Protein Complexes by Electrospray Ionization Mass Spectrometry. *Mass Spectrom. Rev.* **1997,** *16,* 1–23.
29. Loo, J. A. Electrospray Ionization Mass Spectrometry: A Technology for Studying Noncovalent Macromolecular Complexes. *Int. J. Mass Spectrom.* **2000,** *200,* 175–186.
30. Konermann, L.; Simmons, D. A. Protein Folding Kinetics and Mechanisms Studied by Pulse-Labeling and Mass Spectrometry, unpublished.
31. Robinson, C. V.; Chung, E. W.; Kragelund, B. B.; Knudsen, J.; Aplin, R. T.; Poulsen, F. M.; Dobson, C. M. Probing the Nature of Noncovalent Interactions by Mass Spectrometry. A Study of Protein-CoA Ligand Binding and Assembly. *J. Am. Chem. Soc.* **1996,** *118,* 8646–8653.
32. Wu, Q.; Gao, J.; Joseph-McCarthy, D.; Sigal, G. B.; Bruce, J. E.; Whitesides, G. M.; Smith, R. D. Carbonic Anhydrase-Inhibitor Binding—From Solution to the Gas Phase. *J. Am. Chem. Soc.* **1997,** *119,* 1157–1158.
33. Schmidt, A.; Karas, M. The Influence of Electrostatic Interactions on the Detection of Heme–Globin Complexes in ESI-MS. *J. Am. Soc. Mass Spectrom.* **2001,** *12,* 1092–1098.
34. Mauk, M. R.; Mauk, A. G.; Chen, Y. L.; Douglas, D. J. Tandem Mass Spectrometry of Protein–Protein Complexes: Cytochrome c-Cytochrome b_5. *J. Am. Soc. Mass Spectrom.* **2002,** *13,* 59–71.
35. Cunniff, J. B.; Vouros, P. False Positives and the Detection of Cyclodextrin Inclusion Complexes by Electrospray Mass Spectrometry. *J. Am. Soc. Mass Spectrom.* **1995,** *6,* 437–447.

36. Juraschek, R.; Dulcks, T.; Karas, M. Nanoelectrospray—More than just a Minimized Flow Electrospray Ionization Source. *J. Am. Soc. Mass Spectrom.* **1999,** *10,* 300–308.
37. Hu, P.; Ye, Q.-Z.; Loo, J. A. Calcium Stoichiometry Determination for Calcium Binding Proteins by Electrospray Ionization Mass Spectrometry. *Anal. Chem.* **1994,** *66,* 4190–4194.
38. Daniel, J. M.; Friess, S. D.; Rajagopalan, S.; Wendt, S.; Zenobi, R. Quantitative Determination of Noncovalent Binding Interactions Using Soft Ionization Mass Spectrometry. *Int. J. Mass Spectrom.* **2002,** *216,* 1–27.
39. Lee, V. W. S.; Chen, Y.-L.; Konermann, L. Reconstitution of Acid-Denatured Holo-Myoglobin Studied by Time-Resolved Electrospray Ionization Mass Spectrometry. *Anal. Chem.* **1999,** *71,* 4154–4159.
40. Wabnitz, P. A.; Loo, J. A. Drug Screening of Pharmaceutical Discovery Compounds by Micro-Size Exclusion Chromatography/Mass Spectrometry. *Rapid Commun. Mass Spectrom.* **2002,** *16,* 85–91.
41. Evans, S. V.; Brayer, G. D. High-Resolution Study of the Three-Dimensional Structure of Horse Heart Metmyoglobin. *J. Mol. Biol.* **1990,** *213,* 885–897.
42. Hargrove, M. S.; Wilkinson, A. J.; Olson, J. S. Structural Factors Governing Hemin Dissociation from Myoglobin. *Biochemistry* **1996,** *35,* 11300–11309.
43. Adams, P. A. The Kinetics and Mechanism of the Recombination Reaction between Apomyoglobin and Hemin. *Biochem. J.* **1976,** *159,* 371–376.
44. Adams, P. A. The Kinetics of the Recombination Reaction between Apomyoglobin and Alkaline Hematin. *Biochem. J.* **1977,** *163,* 153–158.
45. LaMar, G. N.; Krishnamoorthi. Proton NMR Investigation of the Rate and Mechanism of Heme Rotation in Sperm Whale Myoglobin: Evidence for Intramolecular Reorientation about a Heme Twofold Axis. *J. Am. Chem. Soc.* **1984,** *106,* 6395–6401.
46. Li, Y.-T.; Hsieh, Y.-L.; Henion, J. D.; Ganem, B. Studies on Heme Binding in Myoglobin, Hemoglobin, and Cytochrome c by Ion Spray Mass Spectrometry. *J. Am. Soc. Mass Spectrom.* **1993,** *4,* 631–637.
47. Feng, R.; Konishi, Y. Stepwise Refolding of Acid-Denatured Myoglobin: Evidence from Electrospray Mass Spectrometry. *J. Am. Soc. Mass Spectrom.* **1993,** *4,* 638–645.
48. Hunter, C. L.; Lloyd, E.; Eltis, L. D.; Rafferty, S. P.; Lee, H.; Smith, M.; Mauk, A. G. The Role of the Heme Propionates in the Interaction of Heme with Apo-Myoglobin and Apo-Cytochrome b5. *Biochemistry* **1997**, *36,* 1010–1017.
49. Babu, K. R.; Douglas, D. J. Methanol-Induced Conformations of Myoglobin at pH 4.0. *Biochemistry* **2000,** *39,* 14702–14710.
50. Sogbein, O. O.; Simmons, D. A.; Konermann, L. The Effects of pH on the Kinetic Reaction Mechanism of Myoglobin Unfolding Studied by Time-Resolved Electrospray Ionization Mass Spectrometry. *J. Am. Soc. Mass Spectrom.* **2000,** *11,* 312–319.
51. Simmons, D. A.; Konermann, L. Characterization of Transient Protein Folding Intermediates During Myoglobin Reconstitution by Time-Resolved Electrospray Mass Spectrometry with On-Line Isotopic Pulse Labeling. *Biochemistry* **2002,** *41,* 1906–1914.
52. Clark, S. M.; Leaist, D. G.; Konermann, L. Taylor Dispersion Monitored by Electrospray Mass Spectrometry: A Novel Approach for Studying Diffusion in Solution. *Rapid. Commun. Mass Spectrom.* **2002,** *16,* 1454–1462.
53. Chen, Y.; Yang, J. T.; Martinez, H. M. Determination of the Secondary Structure of Proteins by Circular Dichroism and Optical Rotatory Dispersion. *Biochemistry* **1972,** *22,* 4120–4131.
54. Saxena, V. P.; Wetlaufer, D. B. A New Basis for Interpreting the Circular Dichroism Spectra of Proteins. *Proc. Nat. Acad. Sci. U.S.A.* **1971,** *68,* 969–972.
55. Greenfield, N.; Fasman, G. D. Computed Circular Dichroism Spectra for the Evaluation of Protein Conformation. *Biochemistry* **1969,** *8,* 4108–4116.
56. Nishii, I.; Kataoka, M.; Tokunaga, F.; Goto, Y. Cold Denaturation of the Molten Globule States of Apomyoglobin and a Profile for Protein Folding. *Biochemistry* **1994,** *33,* 4903–4909.
57. Meunier, C.; Jamin, M.; De Pauw, E. On the Origin of the Abundance Distribution of Apomyoglobin Multiply Charged Ions in Electrospray Mass Spectrometry. *Rapid Comm. Mass Spectrom.* **1998,** *12,* 239–245.
58. Bismuto, E.; Colonna, G.; Irace, G. Unfolding Pathway of Myoglobin. Evidence for a Multistate Process. *Biochemistry* **1983,** *22,* 4165–4170.
59. Puett, D. The Equilibrium Unfolding Parameters of Horse and Sperm Whale Myoglobin. *J. Biol. Chem.* **1973,** *248,* 4623–4634.
60. Acampora, G.; Hermans, J. Reversible Denaturation of Sperm Whale Myoglobin. I. Dependence on Temperature, pH, and Composition. *J. Am. Chem. Soc.* **1967,** *89,* 1543–1547.
61. Hargrove, M. S.; Barrick, D.; Olson, J. S. The Association Rate Constant for Heme Binding to Globin is Independent of Protein Structure. *Biochemistry* **1996,** *35,* 11293–11299.
62. Schechter, A. N.; Epstein, C. J. Spectral Studies on the Denaturation of Myoglobin. *J. Mol. Biol.* **1968,** *35,* 567–589.
63. Hargrove, M. S.; Olson, J. S. The Stability of Holomyoglobin is Determined by Heme Affinity. *Biochemistry* **1996,** *35,* 11310–11318.
64. Fersht, A. Structure and Mechanism in Protein Science; W. H. Freeman and Co.: New York, 1999, p 518.
65. Sage, J. T.; Morikis, D.; Champion, P. M. Spectroscopic Studies of Myoglobin at Low pH: Heme Structure and Ligation. *Biochemistry* **1991,** *30,* 1227–1237.
66. Collings, B. A.; Douglas, D. J. Conformation of Gas-Phase Myoglobin Ions. *J. Am. Chem. Soc.* **1996**, *118,* 4488–4489.
67. Taylor, G. Dispersion of Soluble Matter in Solvent Flowing Slowly Through a Tube. *Proc. Roy. Soc. London A* **1953,** *219,* 186–203.
68. Aris, R. On the Dispersion of a Solute in a Fluid Flowing Through a Tube. *Proc. Roy. Soc. London A* **1956,** *235,* 67–77.
69. Vanderslice, J. T.; Stewart, K. K.; Rosenfeld, A. G.; Higgs, D. J. Laminar Dispersion in Flow-Injection Analysis. *Talanta* **1981,** *28,* 11–18.
70. Ruzicka, J.; Hansen, E. H. Flow Injection Analysis, 2nd ed.; John Wiley and Sons: New York, Chichester, Brisbane, Toronto, Singapore, 1988; Vol. LXII.
71. Wuelfing, W. P.; Templeton, A. C.; Hicks, J. F.; Murray, R. W. Taylor Dispersion Measurements of Monolayer Protected Clusters: A Physicochemical Determination of Nanoparticle Size. *Anal. Chem.* **1999,** *71,* 4069–4074.
72. Konermann, L. Monitoring Reaction Kinetics by Continuous-Flow Methods: The Effects of Convection and Molecular Diffusion Under Laminar Flow Conditions. *J. Phys. Chem. A* **1999,** *103,* 7210–7216.
73. Konermann, L.; Rosell, F. I.; Mauk, A. G.; Douglas, D. J. Acid-Induced Denaturation of Myoglobin Studied by Time-Resolved Electrospray Ionization Mass Spectrometry. *Biochemistry* **1997,** *36,* 6448–6454.
74. Corbett, R. J. T.; Roche, R. S. Use of High-Speed Size-Exclusion Chromatography for the Study of Protein Folding and Stability. *Biochemistry* **1984,** *23,* 1888–1894.
75. Goto, Y.; Calciano, L. J.; Fink, A. Acid-Induced Folding of Proteins. *Proc. Natl. Acad. Sci. U.S.A.* **1990,** *87,* 573–577.
76. Johnson, R. S.; Walsh, K. A. Mass Spectrometric Measurementof Protein Amide Hydrogen Exchange Rates of Apo- and Holo-Myoglobin. *Protein Sci.* **1994,** *3,* 2411–2418.
77. Chowdhury, S. K.; Katta, V.; Chait, B. T. Probing Conformational Changes in Proteins by Mass Spectrometry. *J. Am. Chem. Soc.* **1990,** *112,* 9012–9013.

78. Konermann, L.; Collings, B. A.; Douglas, D. J. Cytochrome c Folding Kinetics Studied by Time-Resolved Electrospray Ionization Mass Spectrometry. *Biochemistry* **1997,** *36,* 5554–5559.
79. Konermann, L.; Douglas, D. J. Equilibrium Unfolding of Proteins Monitored by Electrospray Ionization Mass Spectrometry: Distinguishing Two-State from Multi-State Transitions. *Rapid Commun. Mass Spectrom.* **1998,** *12,* 435–442.
80. Konermann, L.; Douglas, D. J. Unfolding of Proteins Monitored by Electrospray Ionization Mass Spectrometry: A Comparison of Positive and Negative Ion Modes. *J. Am. Soc. Mass Spectrom.* **1998,** *9,* 1248–1254.
81. Wagner, D. S.; Anderegg, R. J. Conformation of Cytochrome c Studied by Deuterium Exchange Electrospray Ionization Mass Spectrometry. *Anal. Chem.* **1994,** *66,* 706–711.
82. Loo, J. A.; Edmonds, C. G.; Udseh, H. R.; Smith, R. D. Effect of Reducing Disulfide-Containing Proteins on Electrospray Ionisation Mass Spectra. *Anal. Chem.* **1990,** *62,* 693–698.
83. Kaltashov, I. A.; Eyles, S. J. Studies of Biomolecular Conformations and Conformational Dynamics by Mass Spectrometry. *Mass Spectrom. Rev.* **2002,** *21,* 37–71.
84. Fenn, J. B. Ion Formation from Charged Droplets: Roles of Geometry, Energy, and Time. *J. Am. Soc. Mass Spectrom.* **1993,** *4,* 524–535.
85. GrandoriR. On the Origin of the Conformation Dependence of Protein Charge-State Distributions in Electrospray Ionization Mass Spectrometry. *J. Mass. Spectrom.*, in press.
86. Gumerov, D. R.; Dobo, A.; Kaltashov, I. A. Protein-Ion Charge-State Distributions in Electrospray Ionization Mass Spectrometry: Distinguishing Conformational Contributions from Masking Effects. *Eur. J. Mass Spectrom.* **2002,** *8,* 123–129.
87. Happersberger, H. P.; Stapleton, J.; Cowgill, C.; Glocker, M. O. Characterization of the Folding Pathway of Recombinant Human Macrophage-Colony Stimulating Factor β (rhM-CSF β) by Bis-Cysteinyl Modification and Mass Spectrometry. *Proteins Suppl.* **1998,** *2,* 50–62.
88. Miranker, A. D. Mass Spectrometry of Proteins of Known Mass. *Proc. Natl. Acad. Sci. U.S.A.* **2000,** *97,* 14025–14027.
89. Smith, K. M.Porphyrins and Metalloporphyrins; Elsevier Scientific Publishing Company: New York, 1975 p 804.
90. Oleschuk, R. D.; Harrison, D. J. Analytical Microdevices for mass spectrometry. *Trends Anal. Chem.* **2000,** *19,* 379–388.